The Roded gold occurrence, southern Israel

Ron Bogoch, Moshe Shirav (Schwartz), Aryeh Gilat, and Ludwik Halicz
Geological Survey of Israel, 30 Malkhe Yisrael Street, Jerusalem 95501, Israel

ABSTRACT

Bogoch, R., Shirav (Schwartz), M., Gilat, A., and Halicz, L. The Roded gold occurrence, southern Israel. Isr. J. Earth Sci. 54: 35–45.

Regional and local detailed wadi sediment geochemical exploration led to the discovery of gold-arsenic mineralization in the Neoproterozoic terrain (Nahal Roded area) of southern Israel and the outlining of at least one other potential target. The examined surface and subsurface mineralization (within quartz diorite and gneiss) is wholly within the oxidation zone. Assuming that the present dispersal of the mineralization in the gneiss approximates that of its primary distribution, the deposition was hydrothermal-like and controlled by channelways along fault planes and fissility of the host rock.

The Roded quartz diorite is considered as the source for the gold mineralization. This is similar to an I-type intrusion-related gold system with relatively shallow emplacement depths and mineralogical and geochemical features consistent with the Roded gold occurrence. This model is based on scavenging gold and related metals by a magmatic volatile phase and their transportation to an associated hydrothermal system from which they were deposited to a limited extent within the quartz diorite and in the more amenable surrounding metamorphic country rock.

INTRODUCTION

Three ephemeral stream (wadi) sediment gold anomalies were discovered during a regional multielement geochemical survey of the Precambrian terrain in southern Israel (Bogoch et al., 1993). The gold anomalies occur within or close to exposures of the Roded quartz diorite pluton, some 5 km north of the town of Elat (Fig. 1). A detailed geochemical survey was carried out in the central anomaly (Mount Yedidya) area. Sediment and rock geochemical studies were made to determine possible source rocks, and two boreholes were drilled at a selected site.

This paper presents data on the detailed geochemical survey of the central anomaly, and on the geochemistry, mineralogy, and derivation of the gold-bearing occurrences.

GEOLOGICAL SETTING

The Israeli Precambrian (Neoproterozoic) covers some 70 km^2 in the southern part of the country, and represents part of the northern exposures of the Arabo-Nubian Shield. The area containing the gold anomalies
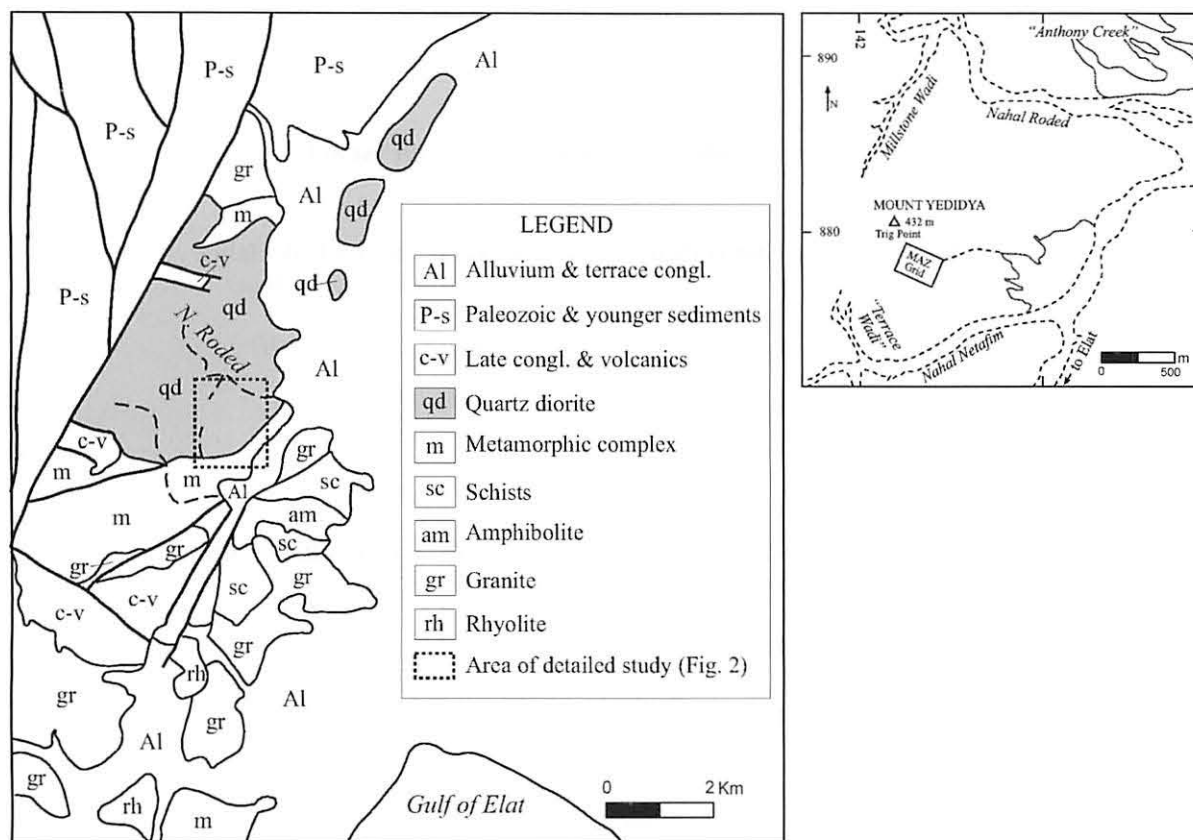
E-mail: ron.bogoch@gsi.gov.il

Fig. 1. Location and schematic geological map of the Roded area (modified after Sneh et al., 1998). Inset, to right, shows location of sites noted in the Mount Yedidya area (Fig. 2) and the "Terrace Wadi" area (Fig. 3).

consists of the southern exposures of the Roded quartz diorite, dated at ~630 Ma (U–Pb zircon, Stein and Goldstein, 1996; Katz et al., 1998), and the metamorphic complex (quartzo-feldspathic gneiss, migmatites, and minor schists) to its south (Fig. 1). The age of these units and of the metamorphic events is not well constrained. The oldest rocks are apparently the quartz-sodic plagioclase-biotite schists, which may be equivalent to schists occurring further to the south (Gutkin and Eyal, 1998). The latter yielded an age of ~800 Ma (Eyal et al., 1991, and sources therein). The age of deformation of the high-temperature metamorphism is not known, although biotite and amphibole separates from adjacent migmatite indicated 720 Ma (Katz, 1997).

Other Neoproterozoic lithologies present include finely crystalline granite bodies within the quartz diorite, small amphibolite bodies at or near the contact between the metamorphic complex and the quartz diorite, numerous dikes varying in composition between rhyolite and basaltic andesite, and patches of volcano-sedimentary conglomerate.

METHODS

Wadi sediment samples were taken in apparently active channels (gravel bars were generally avoided) after removing the upper few centimeters of sediment. The samples were sieved in the field to <1 mm, and to <0.15 mm (<100 mesh) in the laboratory. For the regional geochemical exploration program, a relatively large sampling density (3 samples per km^2) was employed both because of the relatively short metal dispersion train in arid areas and because of the nugget effect in gold exploration (Bogoch et al., 1993). The <100 mesh fraction permits direct analysis without the need for pulverizing. Heavy mineral separates were prepared for selected samples from the 80–150 mesh fraction. To avoid an essentially random rock-sampling program in the anomaly areas, they were first

examined by a detailed wadi sediment survey with sample intervals varying between 10 and 20 m (~300 samples in the central anomaly—Mt. Yedidya).

Two shallow boreholes were drilled at one location using a Longyear wire-line continuous core drill, transported to the site by helicopter. The two holes, drilled of necessity from a single point, were oriented S47°W (DDH MAZ-1) and S63°W (DDH MAZ-2), at 70° to the vertical, reaching downhole depths of 51.5 and 56 m, respectively. The cores were cut lengthwise, and one half was sampled generally in continuous 0.5 m lengths. These were crushed and split into ~100 ml aliquots, pulverized and analyzed for Au.

Samples were analyzed (Geochemical Laboratory, Geological Survey of Israel) for Au, and in certain areas also for As, Bi, and Sb, using atomic absorption (AA) after organic extraction of Au, and using hydride for As, Sb, and Bi. The minimum detection limit for Au is 10 ppb. Selected samples (with both relatively low and high values) were also analyzed by neutron activation (Canada) and fire assay (South Africa). The results of the AA analyses for Au (those reported herein) were approximately 20% below those obtained by fire assay.

Major and trace elements were measured by inductively coupled plasma–atomic emission spectroscopy (ICP-AES) and inductively coupled plasma–mass spectrometry (ICP-MS). For major elements, samples were heated to 1050 °C, fused with $LiBO_2$, and dissolved in HNO_3. For trace elements, samples were sintered with Na_2O_2 and dissolved in HNO_3. Accuracy for major elements is 2% and for trace elements, 10%.

Mineral analyses were made using JEOL 840 SEM with attached Link 10000 energy-dispersion spectrometer (EDS: ZAF4 program) on polished sections (comparison with standard block files).

Wadi sediment anomalies

Three wadi sediment Au anomalies based on gold values >30 ppb in single samples were found in the regional geochemical sampling program. These anomalies ("Anthony Creek", "Millstone Wadi", "Terrace Wadi") are some 3 km apart near Nahal Roded (Fig. 1). Each anomaly was confirmed by a follow-up survey involving 10–15 wadi sediment samples.

The largest anomaly, centered at Mount Yedidya, which also showed more consistent Au values, was chosen for further work. This led to the delineation of sub-anomalies (Fig. 2a, b) based on: (1) the presence in each area of a relatively large number of samples anomalous in Au (>50 ppb for regular samples; >100 ppb for heavy mineral (HM) samples); (2) among the anomalous samples, several contained unusually high quantities of Au (~1 ppm for regular samples; 1–7 ppm for HM samples); (3) correspondence of a pronounced arsenic anomaly in one sub-
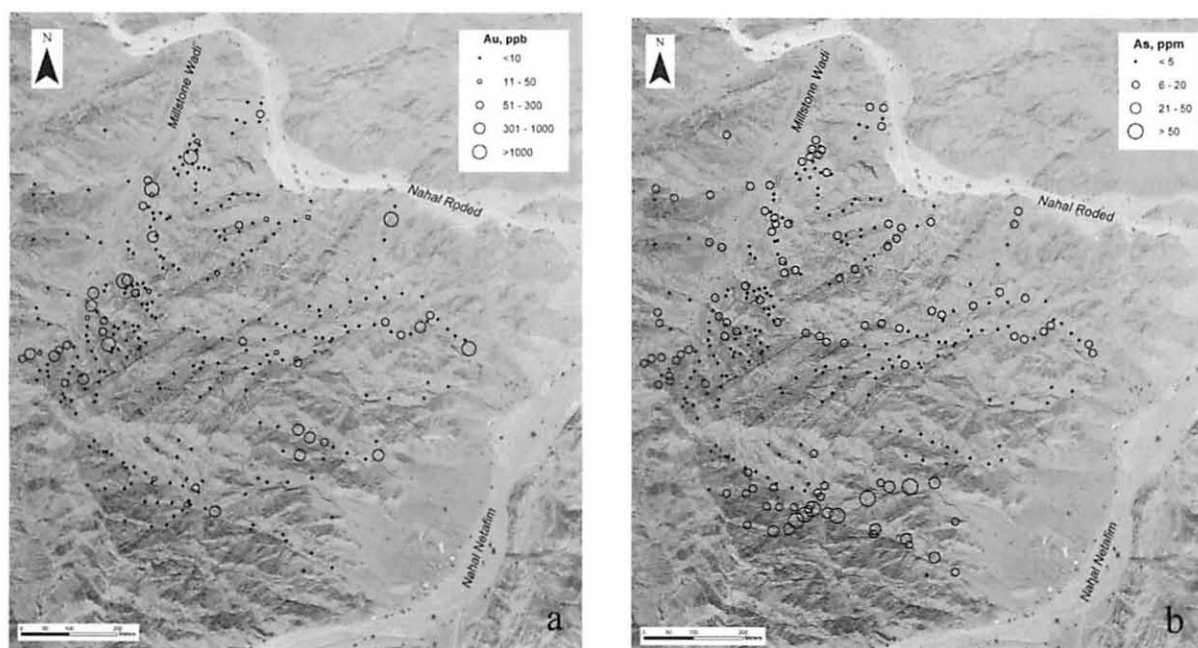

Fig. 2. Wadi sediment geochemical data in the Mt. Yedidya area: (a) Au (ppb) and (b) As (ppm).

anomaly and of antimony in another; (4) their location within a well-defined drainage basin. The sub-anomalies were chosen for a rock geochemical study in an attempt to determine the source of the geochemical anomalies in the sediments.

The "Terrace Wadi" sediment anomaly shows overlapping of Au, As, and Sb in wadi sediment samples concentrated over an area some 400 m in length (NE–SW) and 100 m in width (Fig. 3a–c).

Petrography of the host rocks

Samples of the plutonic body are modally quartz diorite with variations from tonalite to quartz monzodiorite (Bogoch et al., 2002). It is hypidiomorphic to xenomorphic inequigranular (major mineral components 0.5–3 mm). Although it has a rather monotonous appearance in the field, it shows variations in the relative contents of plagioclase (most samples 50–60%), quartz (15–20%), biotite (5–10%), hornblende (4–10%), and K-feldspar (1–3%). The quartz diorite contains hard, dense, generally fine-grained leucocratic granite making up some 5% of the pluton.

The quartzo-feldspathic gneiss at the southern contact with the quartz diorite shows mineralogical, chemical, and field variations. Thus, with the latter, the gneiss varies in nature from linear but poorly foliated, to strongly foliated, to banded. The banding is heterogeneously distributed throughout, although Garfunkel (1980) noted that it is more common closer to the migmatite areas in the west. The gneiss consists of 20–40% quartz, 30–40% sodic to intermediate plagioclase, 10–20% biotite, and 0–15% hornblende. Accessories include titanite, zircon, and apatite.

The migmatites with lesser schists occur to the west of the gneiss. The migmatite melanosome contains quartz, sodic plagioclase, and up to 40% biotite (thin layers very rich in biotite are also present), and the leucosome of quartz and sodic plagioclase with minor biotite. Garnet, sillimanite, and cordierite were recognized in these rocks. The schists consist of sodic plagioclase, quartz, biotite, and some muscovite (Garfunkel, 1980; Gutkin and Eyal, 1998; Katz et al., 1998). The dominant trend of the foliation for the metamorphic rocks is ~N–S and near vertical.

Both magnetic and gravity maps of southernmost Israel indicate that the Roded quartz diorite body is significantly larger in the subsurface (Segev et al., 1999), suggesting that the present exposures represent a relatively high level of the intrusion. Al-hornblende barometry and amphibole–plagioclase thermometry indicate crystallization of the quartz diorite at 2–3 kbar and ~700 °C (Katz et al., 1998).
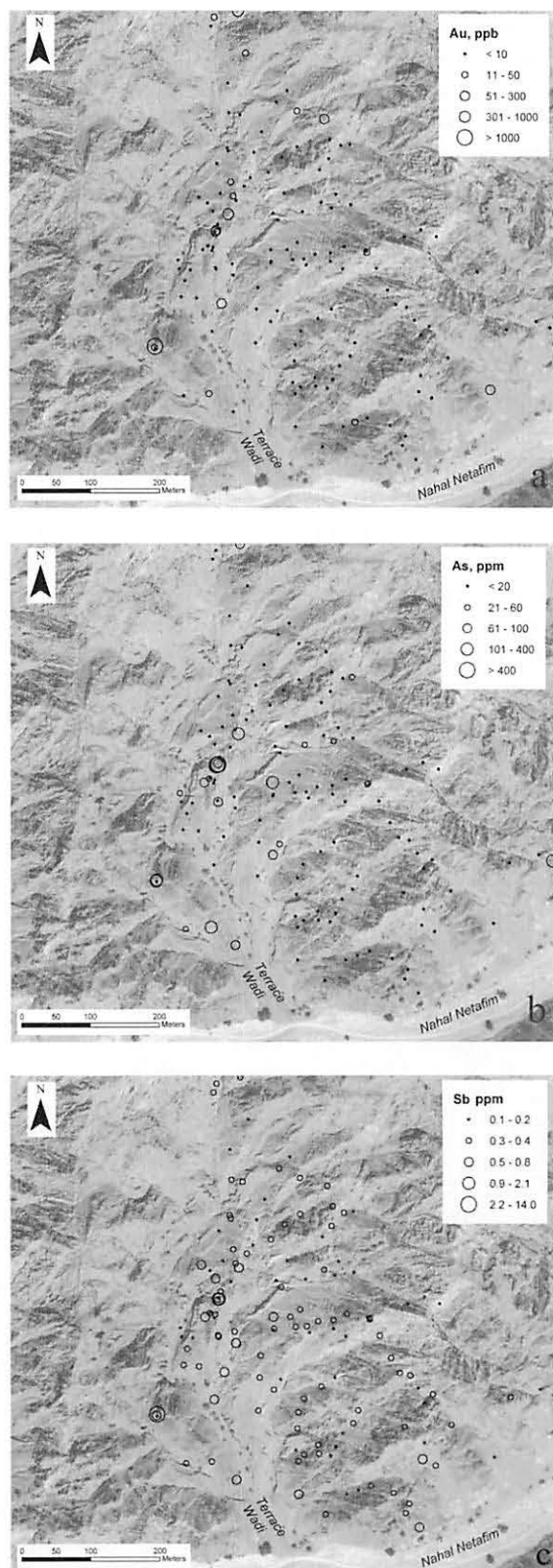

Fig. 3. Wadi sediment geochemical data in the "Terrace Wadi" area: (a) Au (ppb), (b) As (ppm), and (c) Sb (ppm).

MINERALIZATION PHENOMENA

Quartz Diorite

Three of the wadi sediment Au sub-anomalies are contained wholly within quartz diorite, as is the "Anthony Creek" anomaly. Representative samples were taken of all exposed lithologies, apparent alteration zones, dikes, and quartz and carbonate veins within the anomalies. In the quartz diorite, anomalous Au-values (rarely up to 1 ppm) occur within gossan-like Fe-oxide patches and veins generally less than 1 m in maximum length. Locally, quartz veins ranging in width from a few cm to ~0.5 m and in length up to a few meters contain gold in values up to several ppm. The best example of this is a quartz pod of approximately 10 m^2 within the quartz diorite on the southern bank of Millstone Wadi (Fig. 4a) containing up to 9 ppm Au in individual samples. It must be emphasized that these
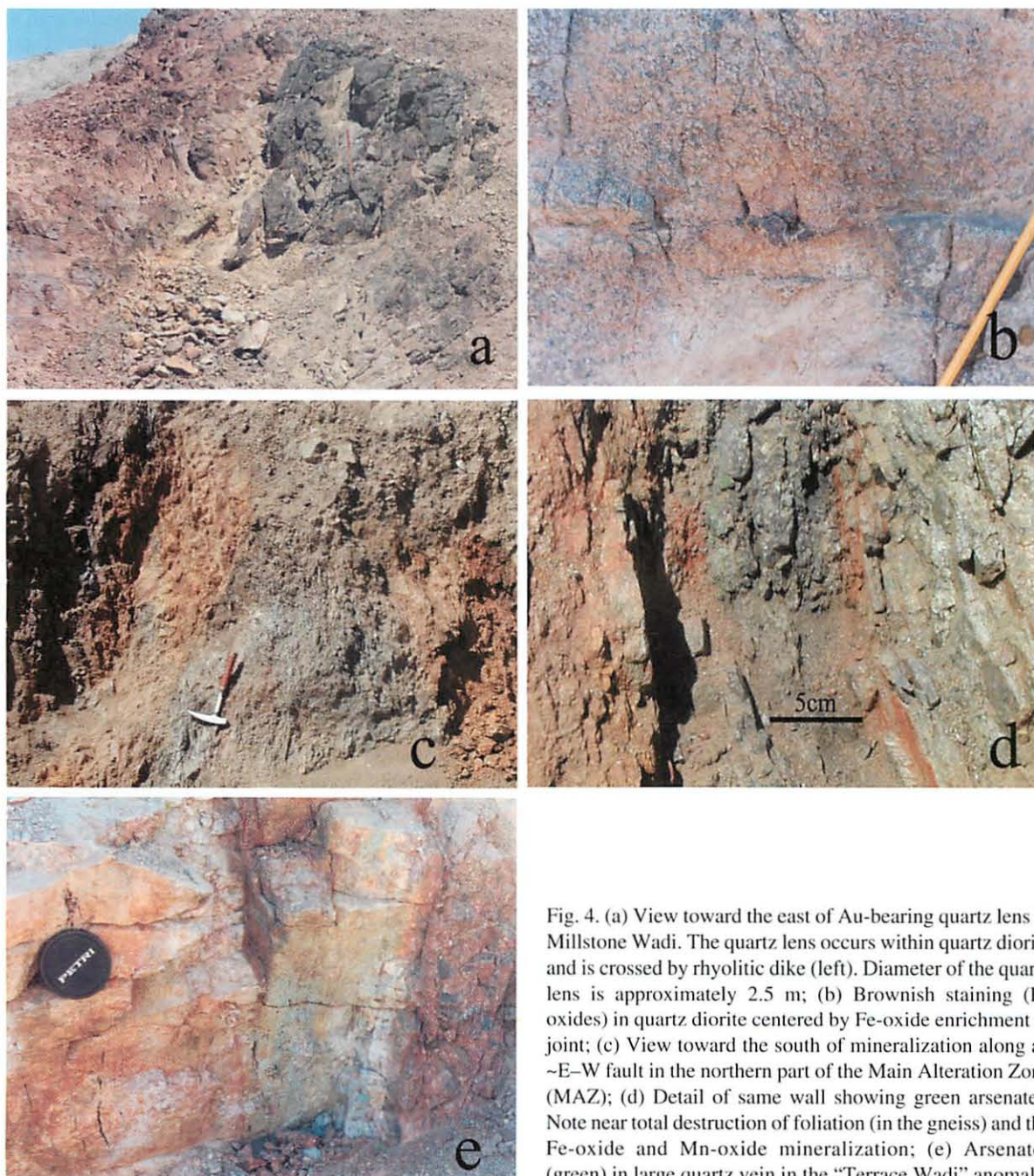
Fig. 4. (a) View toward the east of Au-bearing quartz lens in Millstone Wadi. The quartz lens occurs within quartz diorite and is crossed by rhyolitic dike (left). Diameter of the quartz lens is approximately 2.5 m; (b) Brownish staining (Fe oxides) in quartz diorite centered by Fe-oxide enrichment in joint; (c) View toward the south of mineralization along an ~E–W fault in the northern part of the Main Alteration Zone (MAZ); (d) Detail of same wall showing green arsenates. Note near total destruction of foliation (in the gneiss) and the Fe-oxide and Mn-oxide mineralization; (e) Arsenates (green) in large quartz vein in the "Terrace Wadi" anomaly.

mineralization phenomena in the quartz diorite are not common, and most samples of these materials contained low Au values or were barren. At many locations, there is an overall brownish staining ("limonitic") of the quartz diorite in patches reaching some 100 m² in area, with darker staining along joints (Fig. 4b) (jointing is abundant throughout the pluton). Dust-like scrapings from this stained material locally yielded Au values up to several hundred ppb.

Archaeological sites (~1000 yr BP) are present at two locations of Millstone Wadi, and include partial buildings and numerous millstones constructed of quartz diorite. Quartz-rich comminuted powders located beneath in-situ millstones and in excavated storage facilities contain from ~2 to 8 ppm Au which may have been mined from Au-bearing quartz lenses such as that noted above (Gilat et al., 1993)

Gneiss

The most significant mineralization feature found to date is located in the southernmost sub-anomaly in the Mount Yedidya area, in the area of the significant arsenic anomaly (Figs. 1 and 2) (termed the Main Alteration Zone—MAZ). It consists mainly of iron oxide-rich veins and alteration zones (Fig. 4c), and quartz veins within gneiss, containing clearly visible green arsenates (Fig. 4d), Mn-oxides, and, locally, copper carbonates with chalcocite (Cu_2S) cores (Bogoch et al., 1994). An ~20-m-long sampled section (channel sampled after cleaning the rock face with a jack-hammer) yielded an average of ~0.5 ppm Au, and the area containing this mineralization was examined further based on a 10-m interval grid covering an area of ~150 × 200 m. Some 250 rock samples were taken at the grid points and analyzed for Au, As, and Sb (Fig. 5a–c). The following background values were selected: Au = 20 ppb; As = 60 ppm; Sb = 0.4 ppm. Values above these are considered to be geochemically significant and were used to determine the pattern of mineralization on the surface. Some 30% of the samples contain values above the chosen background. Gold is unevenly distributed through the sampled area, its pattern suggesting the presence of four relatively enriched, sub-adjacent zones with gold mineralization, totaling an area of ~10,000 m². The distribution pattern of samples enriched in As and Sb is very similar to that for the Au, but with broader halos (Fig. 5a–c).

The gold and arsenic mineralization is strongly associated with iron oxides and hydroxides (in places, also quartz), which occur in veins, stringers, and irregular alteration zones. On a local scale, these are in part controlled by the foliation planes in the metamorphic host rock, and the trend of certain of the samples containing >0.5 ppm Au suggests a depositional control by the ~E–W faults as well.

The near-surface mineralization in the MAZ, which is considered to be largely of secondary origin, consists of a suite of arsenates (conichalcite— $CaCuAsO_4(OH)$—Fig. 6a) and plumbian conichalcite (Cu-Ca-Pb arsenate—Fig. 6b), sulfates (gypsum, barite, anglesite, and celestite), phosphate (apatite), iron oxide ("limonite", amorphous to XRD, locally with up to 1% Cu), and silicate minerals (chrysocolla, amorphous Cu–Mn–(Fe–As) silicate, and kaolinite), together with gold (Bogoch et al., 1994). The crystal habit of the latter varies from flat dendritic grains (Fig. 6c), multi-faceted (tetrahahedral?) crystals (Fig. 6d), and spherical 'droplets' (Bogoch et al., 1994) to irregular, in places corroded (primary?) grains. In all occurrences, including that in the quartz diorite, the gold is very fine-grained, rarely reaching 50 μm in diameter.

Results of the gold analyses of cores from the boreholes drilled near the northern boundary of the MAZ are illustrated in Fig. 7. These indicate the presence of several Au-bearing gossan-like zones (in MAZ 1, the downhole interval between 10 and 23 m averages >1.5 ppm). These data suggest that (1) the mineralization uncovered at the surface near the northern part of the MAZ continues to a depth of at least 40 m; (2) the "upper" mineralized zone is fault-controlled, and is some 10 m in width; (3) two "lower" mineralized zones are present, both of apparent narrow width; and (4) the mineralized intervals are in the oxidation zone, which may account for the irregular distribution of Au-values.

Alteration in the mineralized gneiss consists mainly of iron oxide ("limonite"), which fills cracks, forms veinlets, occurs in interstices between minerals, and partially to completely replaces opaque minerals, biotite, and amphibole. The feldspars are strongly sericitized and in places kaolinitized, and the mafic minerals are partially chloritized and epidotized (the latter may not relate to the mineralization). Carbonate is present as stringers and rarely as a replacement product of feldspar. Analyses of representative rock samples from the anomalous areas and boreholes are presented in Table 1. In addition to Au and As, the mineralized gneiss is generally enriched in Sb, Cu, and Pb.

Primary mineralization is absent in the MAZ but may be recorded in the presence of arsenopyrite,

Fig. 5. Geochemistry of rock samples in the MAZ grid. (a) Au (ppb), (b) As (ppm), and (c) Sb (ppm).

Fig. 6. SEM photos of (a) part of aggregate of conichalcite spherulites with radiating acicular blades; (b) Ca–Cu–Pb–arsenate-containing gold crystal; (c) Dendritic Au (in vein quartz); (d) Possible tetrahedral faces of near-equant gold crystals (from conichalcite concentrate). After Bogoch et al., 1994; reprinted with permission from The Mineralogical Society.

Fig. 7. Distribution of Au in boreholes 1 and 2.

Table 1
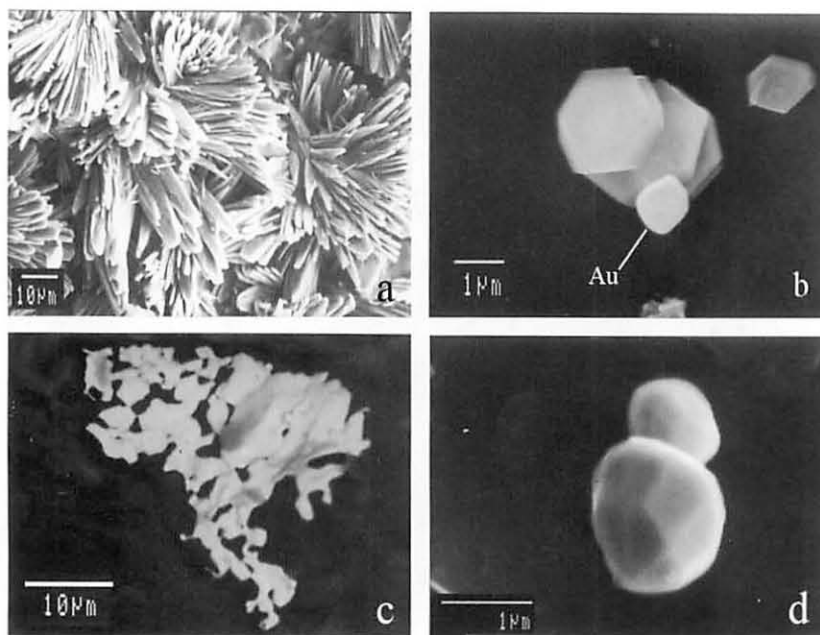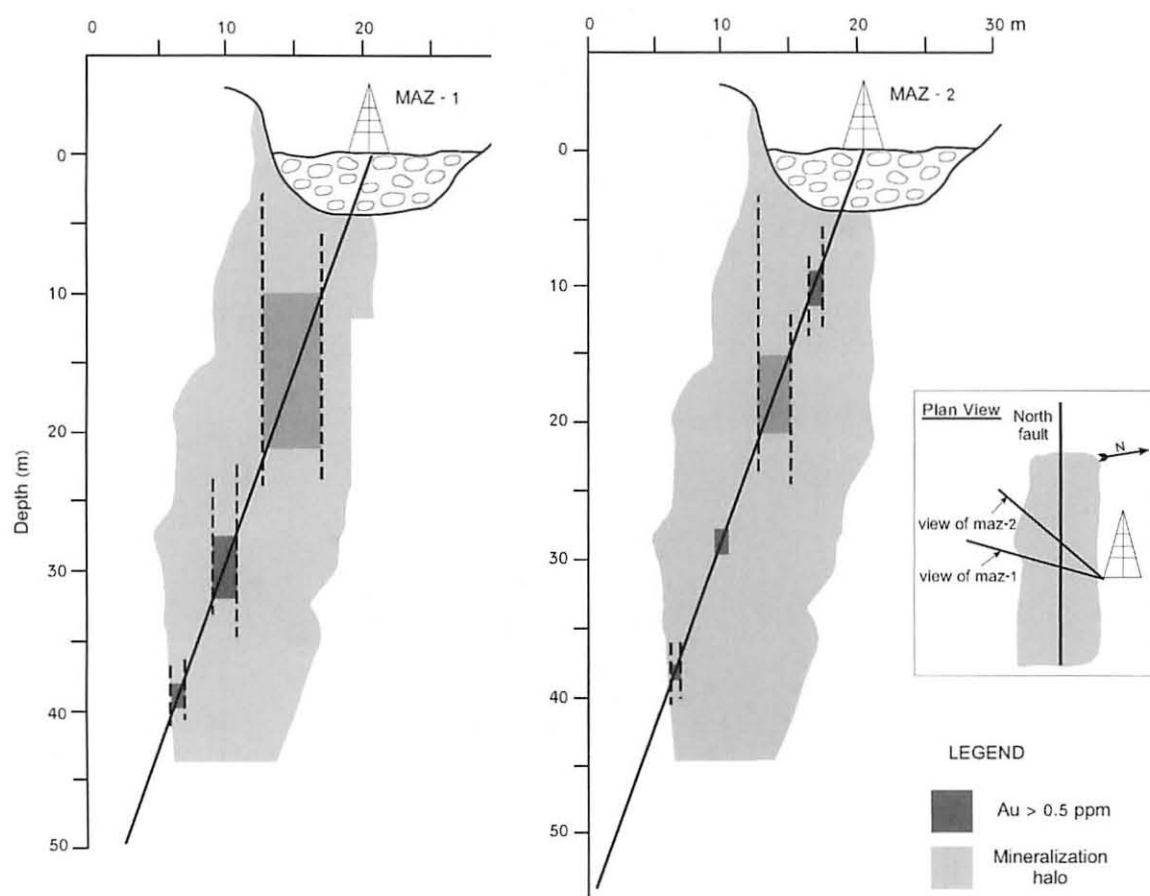Whole rock (wt %) and trace element (ppm, Au in ppb) analyses of representative rock samples from the anomaly areas

	MR-1	MR-2	MR-3	MR-5	MR-19	MR-20	MR-7	MR-8	MR-10	MR-13	MR-16	MR-18
	MAZ	MAZ	MAZ	MAZ	Maz-B	Maz-B	Terrace	Terrace	Terrace	Anth.	Mills.	Mills.
SiO_2	64.6	58.1	58.1	63.7	60.9	62.9	87.8	58.1	67.3	60.2	64.6	95.9
TiO_2	0.6	1.0	0.8	0.9	0.7	0.5	0.1	0.8	0.8	0.8	0.7	<0.05
Al_2O_3	15.8	18.5	16.9	15.9	18.6	16.7	1.4	13.3	15.3	15.8	15.5	0.5
Fe_2O_3	5.7	6.3	6.4	7.0	6.0	5.2	0.9	8.3	5.0	5.7	4.4	3.2
MnO	0.21	<0.05	0.10	0.09	0.10	0.05	<0.05	0.11	0.06	0.07	0.07	<0.05
MgO	3.1	1.0	2.0	2.7	1.3	1.8	0.4	4.4	1.7	4.7	<0.1	<0.1
CaO	0.7	0.6	1.4	1.7	0.6	0.8	4.8	4.7	1.7	4.3	2.7	0.1
Na_2O	3.6	6.7	7.6	3.7	8.5	7.1	0.3	0.7	4.2	4.8	4.9	<0.1
K_2O	2.4	4.1	0.5	1.9	0.8	1.5	0.2	2.9	1.9	1.3	2.1	<0.1
P_2O_5	<0.1	<0.1	<0.1	<0.1	<0.1	<0.1	<0.1	<0.1	<0.1	<0.1	<0.1	<0.1
SO_3	<0.1	0.2	1.4	<0.1	<0.1	<0.1	<0.1	<0.1	<0.1	<0.1	<0.1	0.1
LOI	2.9	2.9	3.9	2.6	2.5	2.6	4.2	6.7	1.2	2.5	2.6	0.5
Total	99.7	99.3	99.1	100.2	100.9	100.3	100.1	100	99.2	100.3	100.9	100.3
Au	1550	4600	350	2000	1100	2500	100	450	<20	200	<20	100
As	1000	2700	2500	250	2500	5600	670	2800	50	5	20	35
Sb	2	7.5	6.5	0.4	4.5	10	17	5.5	0.2	0.2	0.3	0.3
Ag	1	2	2	2	1	1	1	<1	1	1	1	1
Cu	6500	3500	1300	2500	100	120	715	35	26	40	15	155
Pb	12	16	100	11	35	150	23	500	18	6	9	10
Zn	85	40	50	95	120	130	225	440	70	75	75	40
Mo	3	4.5	2.4	1.9	9	6.3	6	5.2	6.7	1.7	2	60
Sn	3.5	2.3	1.3	1.8	0.6	1.7	1.5	3.2	1	1.6	2	80
Be	2	1.5	1.6	2.1	1.3	1.6	0.4	1.8	1.6	1.6	1.7	0.1
Cd	0.2	0.2	0.5	0.1	2.5	3	3	4	0.1	0.2	0.1	2.5
U	2.6	4	6.2	3.2	4.5	10	0.4	2.5	2	1	1.5	0.5
Th	2.8	6.7	5.2	7	6.6	4.9	0.5	2	7.2	2.3	4	0.1
Co	52	13	24	16	17	10	5	26	15	26	22	6
Mn	1800	165	430	670	765	340	260	850	405	585	540	35
Ni	700	16	50	260	50	660	24	65	175	120	390	2000
Cr	275	105	135	220	135	180	400	300	265	270	215	750
V	115	105	75	90	75	65	18	180	70	90	65	15
Ba	525	1300	165	400	180	400	60	285	500	360	635	30
Sr	330	510	380	280	265	320	50	205	280	930	580	40
Y	22	24	24	31	16	11	2.5	23	22	13	11	0.5
La	29	27	27	27	31	13	3.9	8.5	28	19	17	1.2
Ce	54	56	48	52	96	22	6	17	58	43	35	1.8
Pr	7.4	7.3	7.6	7.7	8.9	2.9	0.8	2.7	7.8	6.5	4.7	0.2
Nd	27	26	29	28	31	10	3	11	29	26	18	0.7
Sm	5.1	5.1	6	5.7	5.5	2	0.6	3	5.3	4.5	3.1	0.13
Eu	1.1	1	1.4	1.4	1.4	0.5	0.2	0.8	1.3	1.3	1	0.03
Gd	4.6	4.4	5.4	5.1	4.7	1.8	0.5	3	4.5	3.5	2.5	0.11
Tb	0.68	0.69	0.9	0.84	0.65	0.3	0.07	0.59	0.69	0.48	0.36	0.02
Dy	3.7	4.1	5	5.2	3.4	1.9	0.4	3.8	3.9	2.4	1.9	0.09
Ho	0.72	0.84	0.93	1.07	0.63	0.37	0.07	0.8	0.78	0.44	0.37	0.02
Er	2	2.4	2.5	3.1	1.7	1	0.2	2.2	2.2	1.2	1	0.05
Tm	0.35	0.45	0.41	0.55	0.29	0.19	0.03	0.41	0.38	0.19	0.17	0.01
Yb	2.12	2.76	2.58	3.43	1.81	1.14	0.18	2.5	2.21	1.07	1.09	0.05
Lu	0.29	0.38	0.35	0.46	0.24	0.15	0.02	0.33	0.3	0.14	0.14	0.01

MAZ—Main Alteration Zone (altered gness); Maz-B—Borehole core samples (altered gneiss); Terrace—"Terrace Wadi" anomaly (altered metamorphics and quartz vein); Anth.—"Wadi Anthony" anomaly (Fe-stained quartz diorite); Mill.—Millstone Wadi anomaly (Fe-stained quartz diorite and quartz vein).

chalcopyrite, galena, an unidentified Bi-mineral, and gold within a large quartz vein in the Au–As–Sb anomalous zone in the "Terrace Wadi" anomaly area. This occurs some 300 m W–SW of the MAZ within highly fissile gneiss to schist. Visible surface mineralization consists of conichalcite, mainly with quartz (Fig. 4e). Iron oxide alteration within the metamorphics is similar to that in the MAZ, and contains anomalous gold (up to 1.5 ppm), arsenic (up to 4%), and antimony (up to 14 ppm).

DISCUSSION

The examined surface and subsurface mineralization is wholly within the oxidation zone. The geochemistry together with a local display of sulphides preserved within a large quartz vein, hint at a primary assemblage which included iron (pyrite), copper (chalcopyrite?), arsenic (arsenopyrite), and gold. The lack of silver within the gold is further indicative of gold (re-) deposition under oxidizing conditions. Assuming that the present distribution of the mineralization in the gneiss approximates that of the primary mineralization, the deposition was hydrothermal-like and controlled by channelways along fault planes and fissility of the host rock.

The distribution of the wadi sediment and rock geochemical gold anomalies points to a strong spatial association with the quartz diorite, the latter containing many albeit small occurrences of gold within iron oxide alteration zones. This strongly suggests that the quartz diorite was the source for the gold mineralization and is akin to an intrusion-related gold system (Lang and Baker, 2001), where the intrusions are characteristically I-type, with relatively shallow emplacement depths, contain As, Sb, and Hg (the latter not measured in the present study), with Cu>Pb+Zn, and with clay, quartz, and carbonate alteration (feldspathization occurs at greater depths), and quartz veins (Baker, 2002). These features are consistent with the Roded gold occurrence.

This model is based on the scavenging of the gold and related metals by high-temperature brines (Lang and Baker, 2001) or a magmatic volatile phase (MVP) regardless of sulphur fugacity (Frank et al., 2002). The formation of the fine-grained granite in the Roded quartz diorite was considered by Bogoch et al. (2002) to be related to a late-stage magmatic volatile phase. The MVP exsolved from the magmatic liquid at or close to the site of emplacement possibly due to a decrease in load pressure, and was sufficiently rich in

chloride to act as the scavenging agent of the gold. The MVP further transported the metals to an associated hydrothermal system from which they were deposited to a limited extent within the quartz diorite and in the more amenable surrounding metamorphic country rock.

Au-bearing quartz veins associated genetically with calc-alkaline intrusives have been reported from the Arabo-Nubian Shield in Egypt (e.g., Haraz, 2002), and Saudi Arabia (Albino et al., 1995), and certain of these are presently or were formerly mined.

ACKNOWLEDGMENTS

REFERENCES

Albino, G.V., Jalal, S., Christensen, K. 1995. Neoproterozoic mesothermal gold mineralization at Sukhaybarat East Mine, Saudi Arabia. Inst. Mining and Metallurgy, Trans., Section B: Applied Earth Science 104: 157–170.

Baker, T. 2002. Emplacement depth and carbon dioxide-rich fluid inclusions in intrusion-related gold deposits. Econ. Geol. 97: 1111–1117.

Bogoch, R., Shirav (Schwartz), M., Beyth, M., Halicz, L. 1993. Geochemistry of ephemeral stream sediments in the Precambrian mountainous arid terrain of southern Israel. J. Geochem. Explor. 46: 349–364.

Bogoch, R., Shirav, M., Gilat, A., Halicz, L. 1994. Mineralogy of the near-surface expression of Au-As-Cu mineralization in an arid environment. Min. Mag. 58: 315–323.

Bogoch, R., Avigad, D., Weissbrod, T. 2002. Geochemistry of the quartz diorite–granite association, Roded Area, southern Israel. J. Afr. Earth Sci. 35: 51–60.

Eyal, Y., Eyal, M., Kroener, A. 1991. Geochronology of the Elat Terrain, metamorphic basement, and its implication for crustal evolution of the NER part of the Arabian–Nubian Shield. Isr. J. Earth Sci. 40: 5–16.

Frank, M.R., Candela, P.A., Piccoli, P.M., Glascock, M.D. 2002. Gold solubility, speciation and partitioning as a function of HCl in the brine-silicate melt-metallic gold system at 800 °C and 100MPA. Geochim. Cosmochim. Acta 66: 3719–3732.

Garfunkel, Z. 1980. Contribution to the geology of the Precambrian of the Elat area. Isr. J. Earth Sci. 29: 25–40.

Gilat, A., Shirav, M., Bogoch, R., Avner, U., Nahlielim, D.F.

1993. Significance of gold exploitation in the early Islamic period, Israel. J. Archaeol. Sci. 20: 429–437.

Gutkin, V., Eyal, Y. 1998. Geology and evolution of Precambrian rocks, Mt. Shelomo, Elat area. Isr. J. Earth Sci. 47: 1–17.

Haraz, H.Z. 2002. Fluid inclusions in the mesothermal gold deposit at Atud Mine, eastern desert, Egypt. J. Afr. Earth Sci. Middle East 30: 267–282.

Katz, O. 1997. The metamorphism and structure of the southeastern Roded block. Contribution to the Precambrian basement evolution. M.Sc. thesis, Hebrew Univ., Jerusalem, 102 pp.

Katz, O., Avigad, D., Matthews, A., Heimann, A. 1998. Precambrian metamorphic evolution of the Arabian–Nubian Shield in the Roded area, southern Israel. Isr. J.

Earth Sci. 47: 93–110.

Lang, J.R., Baker, T. 2001. Intrusion-related gold systems: the present level of understanding. Miner. Deposita 36: 477–489.

Segev, A., Goldshmidt, V., Rybakov, M. 1999. Late Precambrian–Cambrian tectonic setting of the crystalline basement in the northern Arabian–Nubian Shield as derived from gravity and magnetic data: basin-and-range characteristics. Isr. J. Earth Sci. 48: 159–178.

Sneh, A., Bartov, Y., Weissbrod, T., Rosensaft, M. 1998. Geological map of Israel, 1:200,000, Sheet 4. Geol. Surv. Isr.

Stein, M., Goldstein, S.L. 1996. From plume head to continental lithosphere in the Arabian–Nubian Shield. Nature 382: 6594, 773–778.